2012

Satellite NDVI Assisted Monitoring of Vegetable Crop Evapotranspiration in California's San Joaquin Valley

Lee F. Johnson

Thomas J. Trout

Remote Sens. **2012**, *4*, 439-455; doi:10.3390/rs4020439

OPEN ACCESS

Remote Sensing

ISSN 2072-4292

www.mdpi.com/journal/remotesensing

Article

Satellite NDVI Assisted Monitoring of Vegetable Crop Evapotranspiration in California's San Joaquin Valley

Lee F. Johnson [1,2,*] and Thomas J. Trout [3]

[1] Division of Science & Environmental Policy, California State University, Monterey Bay, Seaside, CA 93955, USA

[2] Earth Science Division, NASA Ames Research Center, Moffett Field, CA 94035, USA

[3] USDA/ARS Water Management Research Unit, Ft. Collins, CO 80526, USA; E-Mail: Thomas.Trout@ars.usda.gov

* Author to whom correspondence should be addressed; E-Mail: Lee.F.Johnson@nasa.gov; Tel.: +1-650-604-3331; Fax: +1-650-604-4680.

Received: 23 December 2011; in revised form: 21 January 2012 / Accepted: 22 January 2012 / Published: 6 February 2012

Abstract: Reflective bands of Landsat-5 Thematic Mapper satellite imagery were used to facilitate the estimation of basal crop evapotranspiration (ETcb), or potential crop water use, in San Joaquin Valley fields during 2008. A ground-based digital camera measured green fractional cover (Fc) of 49 commercial fields planted to 18 different crop types (row crops, grains, orchard, vineyard) of varying maturity over 11 Landsat overpass dates. Landsat L1T terrain-corrected images were transformed to surface reflectance and converted to normalized difference vegetation index (NDVI). A strong linear relationship between NDVI and Fc was observed (r^2 = 0.96, RMSE = 0.062). The resulting regression equation was used to estimate Fc for crop cycles of broccoli, bellpepper, head lettuce, and garlic on nominal 7–9 day intervals for several study fields. Prior relationships developed by weighing lysimeter were used to transform Fc to fraction of reference evapotranspiration, also known as basal crop coefficient (Kcb). Measurements of grass reference evapotranspiration from the California Irrigation Management Information System were then used to calculate ETcb for each overpass date. Temporal profiles of Fc, Kcb, and ETcb were thus developed for the study fields, along with estimates of seasonal water use. Daily ETcb retrieval uncertainty resulting from error in satellite-based Fc estimation was <0.5 mm/d, with seasonal uncertainty of 6–10%. Results were compared with FAO-56 irrigation guidelines and prior lysimeter observations for reference.

Keywords: crop coefficient; water use; NDVI; Landsat; fractional cover

1. Introduction

In California and much of the western US, municipal, agricultural, and environmental demands increasingly compete for limited water supplies. Continued environmental and regulatory constraints on water supplies in California are anticipated as the effects of population growth, climate change, and declining water conveyance infrastructure continue to evolve. To address these challenges, there is a need to provide new sources of information on crop water use to growers, to enhance their ability to efficiently manage available irrigation water supplies.

California leads the nation in cash farm receipts, and is a major domestic and international supplier of horticultural specialty crops. Such crops, broadly including vegetables, melons, fruits and nuts, generate about 75% of the state's crop sales value [1]. Yet, the growth stages and phenology of many horticultural crops tend to be difficult to generalize due to variations in cultivar, planting density, and cultural practice. Growth stage and crop size are important because canopy light interception is a primary determinant of crop water requirement.

Estimates of crop evapotranspiration (ETc) can support efficient irrigation management. ETc represents the combined processes of crop transpiration and evaporation from the soil surface. A common approach to irrigation scheduling is to calculate ETc by applying a crop coefficient (Kc), which is a dimensionless value generally of range 0.1–1.2, to reference evapotranspiration (ETo), which captures the effect of weather on the atmosphere's evaporating power. The California Irrigation Management Information System (CIMIS) automated weather station network provides daily ETo values, which estimate ET from a well-watered grass surface, gridded across the entire state at 2 km resolution [2,3]. The resulting ETc can help irrigation managers schedule irrigation timing and quantity. Guideline Kc values are available for several crops under idealized phenology expressed as four growth stages (initial, development, mid-season, late-season), as from the FAO-56 procedures [4]. The initial stage is associated with crop emergence and establishment, generally running from planting date to about 10% ground cover. During the ensuing development stage, the crop grows to its maximum cover and Kc. The mid-season stage is a sustained period at maximum Kc, followed by a late-season stage that, depending on crop type, may continue at maximum Kc or may decline due to crop senescence. It should be noted that FAO-56 and other tabulations, however valuable, are intended as a general guide. Actual crop development and water use in a field depends on planting configuration and cultural practice, as well as climatic condition, thus local observations of plant stage development are recommended where possible.

Canopy light interception is a main driver of ETc and hence Kc. Fractional green canopy cover (Fc) is a readily measured property that is a good indicator of light interception. As such, accurate and efficient estimation of actual Fc might allow improved scheduling and allocation of irrigation water [5–8]. Several studies have related Fc, or the closely related metric, fractional ground shaded area, to specialty crop water use [9–14]. This paper is largely based on a multi-year USDA study in the San Joaquin Valley (SJV) that used a weighing lysimeter, which provides the most accurate measure

of daily crop water use, to relate Fc to Kcb for several key vegetable crops: broccoli, bellpepper, head lettuce, and garlic [15]. These crops together, account for about 25% of the state's vegetable acreage and revenue. As is becoming more common in commercial operations, subsurface drip irrigation was used after the initial (crop establishment) growth stage. Water was applied directly to the root zone in small (2 mm) quantities several times a day to avoid surface wetting and associated direct evaporation from the soil surface. In this way, the lysimeter study measured water use relating primarily to plant transpiration. Strong relationships were observed between Fc, which was measured periodically during each growing season, and basal crop coefficient (Kcb), which represents ET of an unstressed crop on a dry soil surface. Kcb maximum values per crop were close to FAO specifications. The purpose of the lysimeter study was to improve irrigation management of vegetable crops, and the possibility of achieving of full yield potential with reduced water was established in some cases.

Additional studies have shown that various spectral vegetation indices, calculated from visible and near-infrared (NIR) reflectance data, are linearly related to canopy light interception [16–22]. Additional research in SJV shows a strong relationship between Landsat normalized difference vegetation index (NDVI) and Fc for multiple horticultural crops [23]. As such, it appears that indices such as NDVI can potentially track canopy development and light interception.

A remote sensing approach, implemented in regions with an available ETo network, potentially enables timely estimation of crop water use for resource monitoring and irrigation scheduling [24]. A key advantage of remote sensing is the ability to directly observe crop development, hence negating the need for idealized growth stage assumptions. This study had two primary research objectives. Objective 1 characterized the relationship between satellite NDVI and fractional cover of major SJV crop types. The SJV is a highly diverse agricultural region, and definition of a generalized NDVI-Fc relationship was intended to support further research into applications that require crop development data. Objective 2 provided an example use of such observations in support of crop evapotranspiration estimation. Under this objective, NDVI imagery was combined with prior lysimeter-based equations and CIMIS ETo data to track crop development and water use of several SJV commercial vegetable fields.

2. Methods

2.1. Study Area

This study included fields located on five large commercial farms in the San Joaquin Valley, in the vicinity of Five Points, California (36.43°N, 120.1°W) (Figure 1). The farms produce a variety of annual and perennial specialty crops. Soil textures in the area range from sandy loam to clay loam soils and all soils were light colored with low organic matter (less than 0.5%). Measured fields were primarily drip irrigated, though sprinkler and furrow systems were represented as well. The fields were mostly weed free. Row orientation in all fields was north-south. All fields were located within 25 km of the University of California's West Side Research and Extension Center (UC-WSREC), where the lysimeter measurements of [15] were made.

Figure 1. Study area. Polygons show fields used for objective #1 (NDVI-Fc relationship). Fields designated as A-J used for objective #2 (crop cycle monitoring) (see also table in Section 2.4). Location of WSREC lysimeter shown for reference.

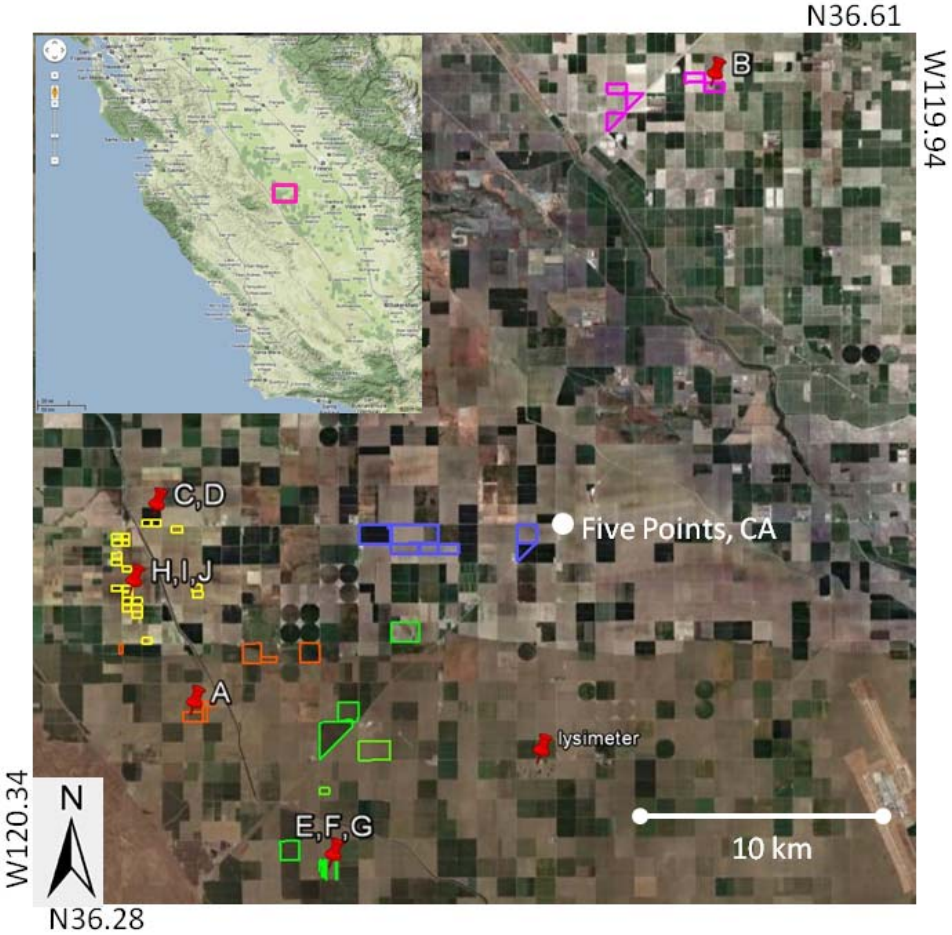

2.2. Landsat Processing

Landsat-5 TM L1T terrain-corrected scenes were collected through the period day-of-year (DOY) 047-319, 2008, sky conditions and instrument operation permitting. The scenes were atmospherically corrected to surface reflectance using software developed under the Landsat Ecosystem Disturbance Adaptive Processing System [25], which incorporated the 6S atmospheric radiative transfer modeling approach [26]. Required inputs included ozone concentration derived from the Total Ozone Mapping Spectrometer, column water vapor and surface pressure from the National Centers for Environmental Prediction Reanalysis Data, and aerosol optical depth estimated by the dark-dense-vegetation method [27]. Red and near-infrared band reflectances were then used to calculate NDVI ((NIR−red)/(NIR+red)) at Landsat TM 30 m spatial resolution.

2.3. Objective 1: Characterization of NDVI-Fc Relationship

Under Objective 1, a total of 74 ground-based measurements of Fc were made in several commercial fields on several Landsat-5 overpass dates (path 42, row 35) during the period DOY 095-287, 2008 (Table 1, column 3). A wide variety of crops and maturity levels were included: lettuce (n = 17), tomato (4), safflower (5), wheat (1), onion (4), barley (1), garlic (1), sugar beet (1), grape (5),

bellpepper (5), cotton (3), corn (1), almond (1), alfalfa (2), pistachio (4), cantaloupe (5), watermelon (3), and broccoli (11). Five observations had wet conditions for a portion of the soil surface. Of these,

Table 1. Landsat-5 TM scenes used for Objective 1: Development of NDVI-Fc relationship (column 3), and Objective 2: Crop-cycle monitoring (column 4).

DOY	Path/Row	NDVI-Fc	Crop cycle	Notes[a]
47	42/35		●	
54	43/35			c
63	42/35		●	
70	43/35		●	
79	42/35		●	
86	43/35		●	
95	42/35	●	●	
102	43/35		●	
111	42/35	●	●	
118	43/35		●	
127	42/35			x
134	43/35		●	
143	42/35	●	●	
150	43/35		●	
159	42/35	●	●	
166	43/35		●	
175	42/35	●	●	
182	43/35		●	
191	42/35	●	●	
198	43/35		●	
207	42/35	●	●	
214	43/35		●	
223	42/35		●	f
230	43/35		●	
239	42/35	●	●	
246	43/35		●	
255	42/35	●	●	
262	43/35		●	
271	42/35	●	●	
278	43/35			c
287	42/35	●	●	
294	43/35		●	
303	42/35		●	
310	43/35			c
319	42/35		●	

[a]c = cloud cover, x = sensor malfunction, f = no Fc ground data collected.

three fields had moist strips aligned with drip emitters and two had wet furrow strips. A ~200 m × 200 m measurement zone was established on the interior of each field, while avoiding field edges. A

"handheld" Agricultural Digital Camera (TetraCam Inc., Chatsworth, CA, USA) was suspended from a frame directly above the crop and aimed vertically downward. The camera was situated 2.3 m above the ground surface for low-growing annual crops (<0.6 m height) and 6.1 m above ground surface for taller perennial crops (vineyards and immature orchards) (Figure 2). Photographs were taken at three approximately evenly spaced locations per zone. Image editing software was used to segment each photo into green vegetation and "other" components (soil background, dry vegetation) based on user-defined spectral thresholds. Percent of pixels representing green vegetation (Fc) was calculated after scaling for row and plant spacing where applicable. Results from the three photos were averaged to derive zone Fc. A GPS reading was recorded within the zone.

The measurement zones were subsequently identified in the NDVI imagery using the GPS coordinates, and confirmed by high resolution Google-Earth imagery. Mean Landsat NDVI values were calculated for a 7 × 7 pixel window centered on the measurement zone and wholly contained within the field boundaries.

Figure 2. Measurement of green fractional cover (Fc) for low and high stature crops using multispectral camera.

2.4. Objective 2: Crop Cycle Monitoring

Under Objective 2, crop-cycle monitoring was retrospectively performed on ten fields containing the vegetable crops used in the earlier USDA lysimeter study: lettuce, broccoli, bellpepper, and garlic. Row spacing and plant populations present in the fields were similar to those used in the lysimeter study. The study area was located in the overlap zone between satellite paths 42 and 43, enabling Landsat-5 observation on 7–9 d intervals (Table 1, column 4). The fields used for this analysis ranged in size from 5–30 ha. Table 2 provides field locations and crops, along with estimated start of crop development stage (rapid NDVI increase) and harvest dates (NDVI decline or drop-off) derived by inspection of satellite temporal profiles.

The autumn crop of lettuce in SJV is typically planted late August or September and harvested late October-early November. Broccoli is planted about the same time, but has a longer growth cycle and is harvested early December. Peppers are planted in spring and harvested during late July or August. These three crops are typically fully irrigated up to harvest, which occurs at or near peak Fc and before significant leaf senescence occurs. Cloud cover after DOY 319 precluded harvest date estimation for the broccoli fields (E, F, G) and one of the lettuce fields (H). Thus, Landsat profiles for these fields represent incomplete crop cycles. The remaining crop, garlic, is typically planted in early winter,

develops rapidly in springtime, and is harvested in summer. Irrigation is discontinued at bulb development in late spring, causing foliar senescence and consequent decline in Fc prior to summer harvest.

Table 2. Fields used for crop-cycle monitoring, with satellite image based estimates of development stage start and harvest day-of-year. Harvest date uncertainty for fields C, D, I, and J was due to lack of cloudfree satellite imagery.

Field	Crop	Size (ha)	Lat (N)	Long (W)	Development (DOY)	Harvest (DOY)
A	garlic	30	36.358	120.270	47	214
B	garlic	30	36.591	120.030	47	214
C	bellpepper	10	36.430	120.291	150	214–223
D	bellpepper	10	36.430	120.286	143	214–223
E	broccoli	5	36.302	120.211	262	>319[a]
F	broccoli	5	36.302	120.209	255	>319[a]
G	broccoli	5	36.302	120.204	246	>319[a]
H	lettuce	10	36.400	120.300	262	>319[a]
I	lettuce	10	36.406	120.304	255	303–319
J	lettuce	10	36.404	120.300	262	303–319

[a]incomplete growth cycle.

Mean NDVI was extracted for each field on each clear-sky satellite overpass date. The NDVI values were then converted to Fc based on a relationship defined by research objective 1, and subsequently to Kcb by prior lysimeter results (Table 3). Finally, Kcb was multiplied by ETo for each specific field location and date, as extracted from the 2 km Spatial CIMIS archive, to retrieve basal (or, potential) crop evapotranspiration (ETcb). Typically, ETo values within the study area range from approx. 1 mm/d in winter to just over 7 mm/d in summer (Figure 3). The ETcb values were integrated from beginning of crop development stage through harvest to estimate seasonal water use in each field.

Table 3. Equations relating Fc to basal crop coefficient (Kcb) for four vegetable crops, after USDA weighing lysimeter experiments [15]. The Fc was measured periodically during each growing season by ground methods similar to those reported above in Section 2.3. Response functions for lettuce and bellpepper were nearly linear for Fc ranging up to about 0.8. The garlic and broccoli functions are more curvilinear with asymptotic behavior at Fc beyond 0.8. See also Figure 8 of [15].

Crop	Conversion Equation	Reported r^2
garlic	$Kcb = -0.985Fc^2 + 1.759Fc + 0.272$	0.992
bellpepper	$Kcb = -0.078Fc^2 + 1.124Fc + 0.142$	0.994
broccoli	$Kcb = -0.933Fc^2 + 1.756Fc + 0.181$	0.999
lettuce	$Kcb = -0.07Fc^2 + 1.08Fc + 0.209$	0.992

Figure 3. Historical average daily reference evapotranspiration (ETo) for study area, exemplified by data from the CIMIS Five Points station at UC-WSREC. Note seasonality effect, with higher values in summer.

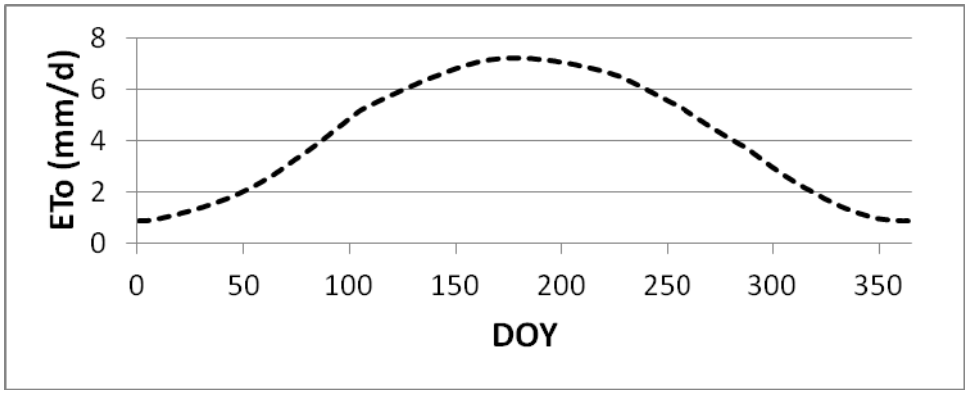

3. Results and Discussion

3.1. Relationship between NDVI and Fc

Ground observations of Fc were made across 49 fields planted to 18 different crops (including row crops, grains, orchard, vineyard) of varying maturity, over 11 satellite overpass dates (Table 1, Column 3). Mature orchards were excluded due to difficulty positioning the camera at sufficient height above very tall canopies; the most mature orchard included here was 3rd-year pistachio, with ~2.5 m tree height and measured Fc of 0.35. Full dataset Fc ranged from 0.01 to 0.97 and NDVI from 0.12 to 0.88. To first approximation, Fc observations can be regarded as a linear mixture of canopy and bare soil spectra. Indeed, a strong linear relationship was observed between the two variables (r^2 = 0.96, RMSE = 0.062, $p < 0.01$) (Figure 4). The trendline equation was:

$$Fc = 1.26(NDVI) - 0.18 \quad (1)$$

Past studies have identified several factors that can contribute to scatter in the observed relationship. Higher leaf area per unit ground area within the canopy will, to a point, cause elevated NDVI per given Fc. Such differences can be substantial between annuals and perennials. An increase in proportion of exposed soil that is shaded by vegetation will elevate NDVI per Fc, an effect that might be expected greater for taller crops. The presence of wet (darker) soil will similarly elevate NDVI. Differences in leaf optical properties in the red and NIR will modify canopy NDVI and introduce noise. All of these factors would be expected to be problematic when comparing across multiple plant species, fields, maturity levels, and dates. In spite of these possible sources of variability, the reasonably low RMS error indicates that NDVI is a robust indicator of crop Fc.

The overall relationship (Equation (1)) was in good agreement with prior analyses reported for individual crop types (Figure 5). The positive x-intercept seen for all relationships is due to the fact that bare soils are typically somewhat brighter in the NIR than in the red [28], producing mildly positive NDVI. A trendline limited to the four crops addressed here was not significantly different from the pooled relationship, thus Equation (1) was used for subsequent NDVI-Kcb transformations under Objective 2.

Figure 4. Relationship between Landsat NDVI and ground measurements of Fc. A total of 18 major SJV crop types and 11 satellite overpasses are represented. Number of observations of each crop type shown in parentheses.

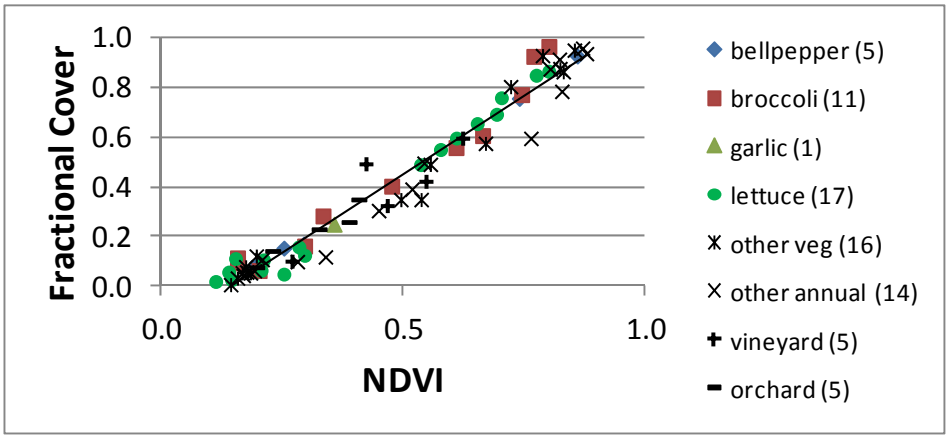

Figure 5. Comparison of Equation (1) with published relationships for multiple horticultural crops [23], wheat [21,22], barley [19], and grape [20]. Each line covers approximate data range of respective study.

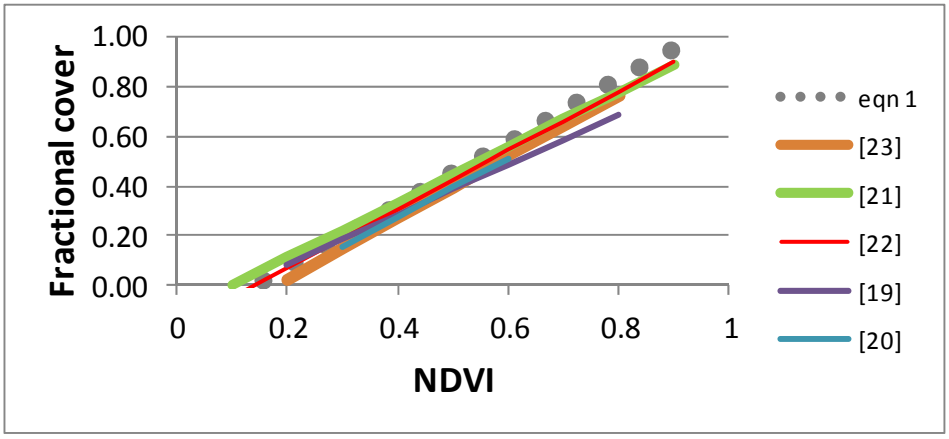

3.2. Fc Profiles

Mean NDVI time-series were extracted for the respective growth-cycles (less initial crop stage) of the Table 2 study fields. Equation (1) was used to convert the NDVI observations to Fc (Figure 6). The resulting profiles reveal differences in phenology and development rate among fields. The broccoli profiles show clear differences in development start, apparently due to staggered planting dates, yet all attain the same maximum Fc (about 0.95) by DOY 319. The lettuce profiles suggest that field I was planted prior to fields H and J, that field J developed more rapidly than the others, and that all fields reached approximately the same maximum Fc by DOY 303. The bellpepper fields were phenologically similar and both reached maximum Fc of about 0.82, yet field D showed greater cover throughout much of the development stage. The garlic fields were phenologically similar as well. Field B had greater cover for most of the cycle, although both attained about the same peak near 0.7. Excepting garlic, the satellite profiles were in good agreement, both in amplitude and timing, with ground-based Fc measurements taken periodically during the lysimeter experiments. For garlic, the satellite Fc

estimates suggest that the study field phenologies were somewhat delayed and growth ultimately less vigorous than the lysimeter crop. The eventual dramatic Fc decline suggests that harvest occurred between DOY 214-223 for bellpepper and 303-319 for lettuce fields I, J. Estimated harvest date for garlic, DOY 214, was assumed to follow total senescence of above-ground biomass as per typical management of this crop [29]. End of season satellite data for lettuce field H and broccoli fields (E,F,G) were unavailable due to cloud cover.

Figure 6. Landsat time-series of mean Fc beginning at apparent start of development stage for four different crops, with trendlines. Letters represent fields of Table 2. Observed profiles for fields E, F, G, and H terminate prior to harvest due to cloud cover past DOY 319. Full growth cycle captured for the other fields. The trendlines exclude the final plotted datapoints for fields C, D, I, and J, which represent apparent post-harvest conditions and are shown for reference only. Fc measurements obtained during respective lysimeter experiments [15] also shown for reference.

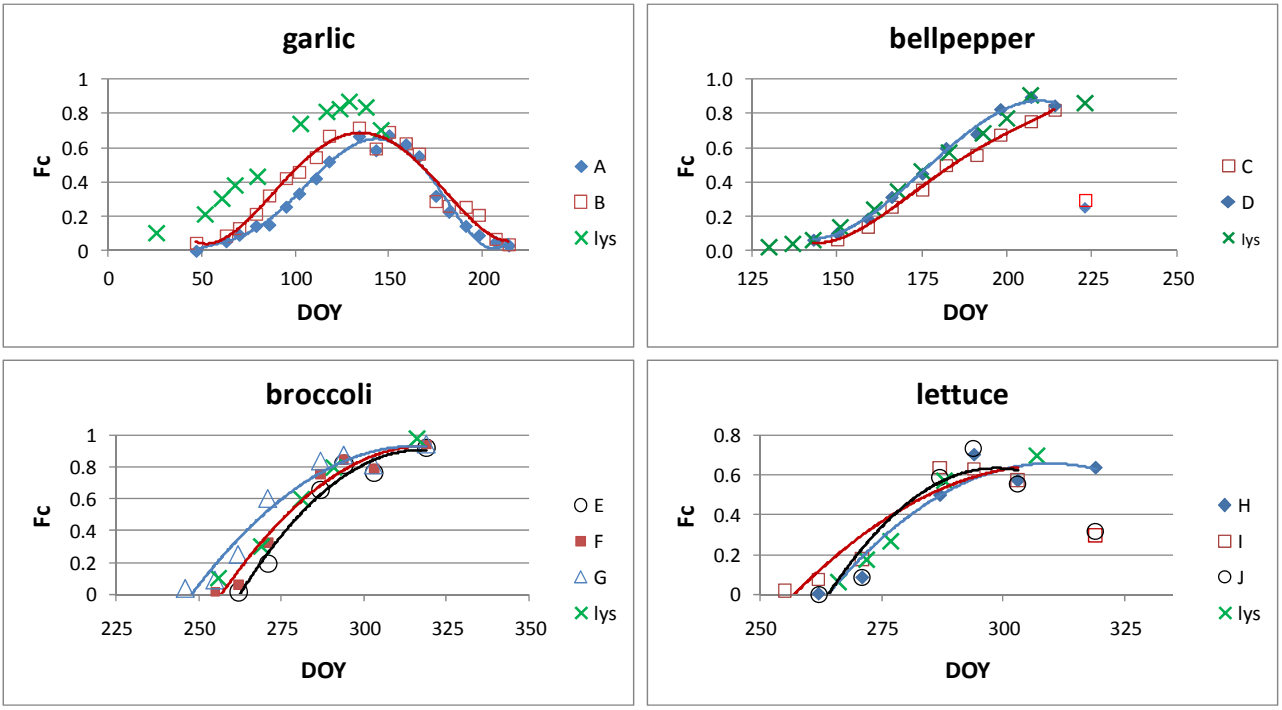

3.3. Kcb and ETcb Profiles

The Fc datapoints were converted to Kcb (Figure 7) based on the lysimeter equations of Table 3. Basal crop coefficient profiles from FAO-56 planning guidelines, excluding the initial crop stage, are provided for comparison. The lettuce fields followed the FAO-56 guideline fairly closely during the development stage, reaching a peak Kcb of about 0.9. Notably, however, fields I and J showed a much faster total crop cycle (respective maxima of 64 and 57 d, *vs*. 75 d for guideline) while field H duration was inconclusive due to cloud cover. The broccoli fields developed at a somewhat faster rate than the guideline, and total duration was inconclusive. Peak Kcb (near 1.0) slightly exceeded the guideline maximum of 0.95. For bellpepper, the fields developed at a markedly slower rate (about 70 d) than guideline (35 d), though at a similar rate to that reported in the lysimeter study. Neither field showed a

pronounced mid-season stage. Peak Kcb near 1.0 was in good agreement with guideline. As with lettuce, crop cycle duration (maximum 73 d) was much shorter than the guideline (95 d). The FAO-56 guideline does not provide stage durations for garlic and hence this crop could not be compared in the same fashion, though it does specify a maximum Kcb of 0.9 (not shown) *vs*. observed peak near 1.0.

Figure 7. Landsat based time-series of Kcb for four different crops, with trendlines. Letters represent fields of Table 2. Dashed line is planning guideline for crop development, mid-season, and late-season stages from FAO-56 Tables 11 and 17 [4] as available (FAO does not provide stage duration for garlic.). FAO development stage start dates were roughly aligned with observed dates for comparison purposes.

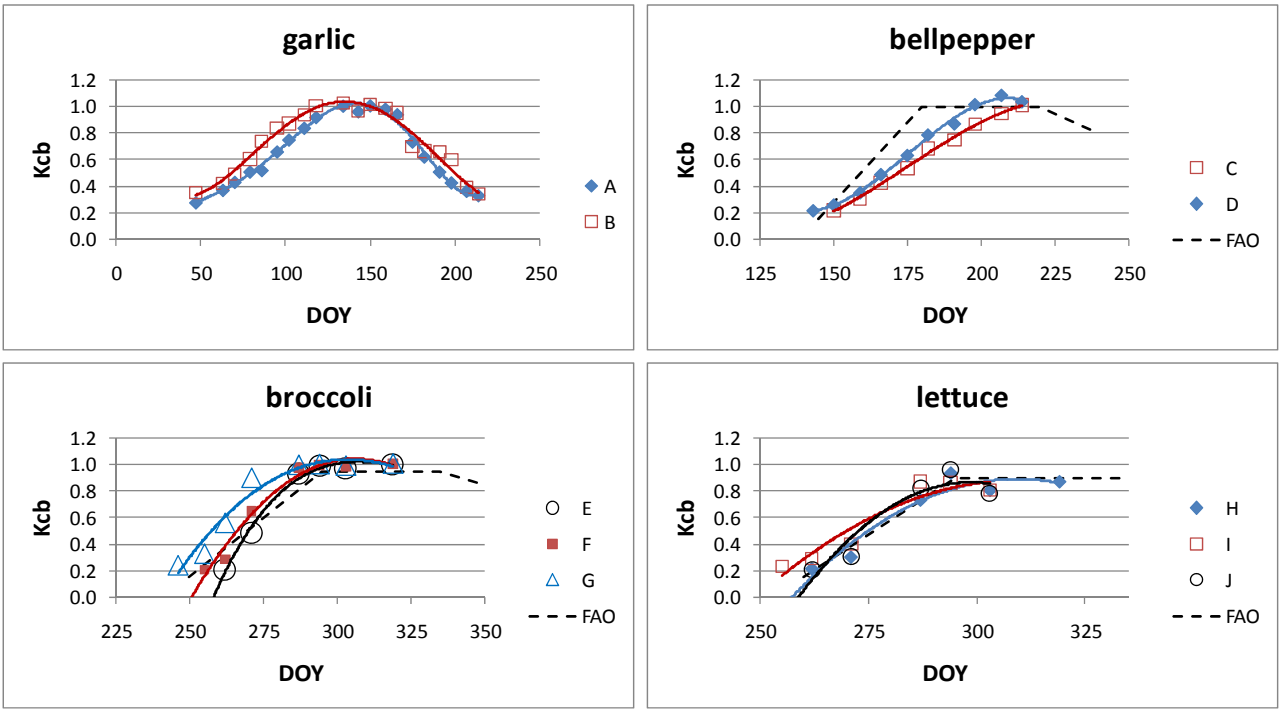

The Kcb trendlines were used to estimate Kcb per field on each day of the observed crop cycle. These daily values were multiplied by 2008 Spatial CIMIS ETo to generate daily ETcb. Summary indicators of crop water use were subsequently developed to include mean, minimum and maximum daily ETcb and total cumulative ETcb values (Table 4), and cumulative ETcb time-series (Figure 8). The ETcb values are highly sensitive to prevailing ETo, which varies widely throughout the year (Figure 3). Garlic and bellpepper matured at a time of high evaporative demand (summer) and thus have greater daily ETcb mean and maximum values than the autumn broccoli and lettuce crops. Cumulative ETcb is sensitive to crop duration as well, and fields with longer growth stages tend to show higher total water use.

From Figure 8, it can be seen that total ETcb for lettuce fields I and J fell between the lysimeter crop and FAO-56. Cumulative water use profiles for broccoli show clear differences in timing, reflecting apparent offsets in planting date. Though all of the broccoli profiles are incomplete, total ETcb for field G already exceeds the FAO full season value, as does the final value for the lysimeter crop. For bellpepper, consistent with the Fc profiles, cumulative ETcb of fields C and D lagged FAO. Total ETcb was markedly lower than FAO yet was in the lower range shown by the lysimeter crop.

Bellpepper is an indeterminate crop, meaning that it bears fruit, and can be repeatedly harvested, over an extended period of time. Due to this, comparison of total ETcb values can be problematic. The satellite Fc profiles suggest that study fields C and D were harvested all at once, which is typical of processing peppers under mechanical harvest, and that the plants were then disked in order to cut ET and reduce insect and disease issues. The lysimeter fields were hand-harvested over a prolonged period, while the FAO guideline is ambiguous on this point. Data are presented for the garlic fields from start of development stage until approximate time of irrigation shutdown. As was previously noted, these fields lagged the lysimeter crop in phenology and ultimate vigor, and these trends are reflected in terms of lower cumulative ETcb.

Figure 8. Cumulative basal evapotranspriation (ETcb) for four different crops, excluding initial stage, developed by lysimeter equations (Table 3) constrained by satellite-based Fc, and combined with CIMIS reference evapotranspiration. Letters represent fields of Table 2. Dotted portions of bellpepper (C,D) and lettuce (I,J) lines represent harvest period. Garlic profiles terminate at irrigation cutoff. Lysimeter [15] and FAO profiles are provided for reference as available. Dashed portion of the lysimeter line for bellpepper represents reported harvest period. Satellite-based profiles for fields E, F, G, and H are incomplete due to cloud cover.

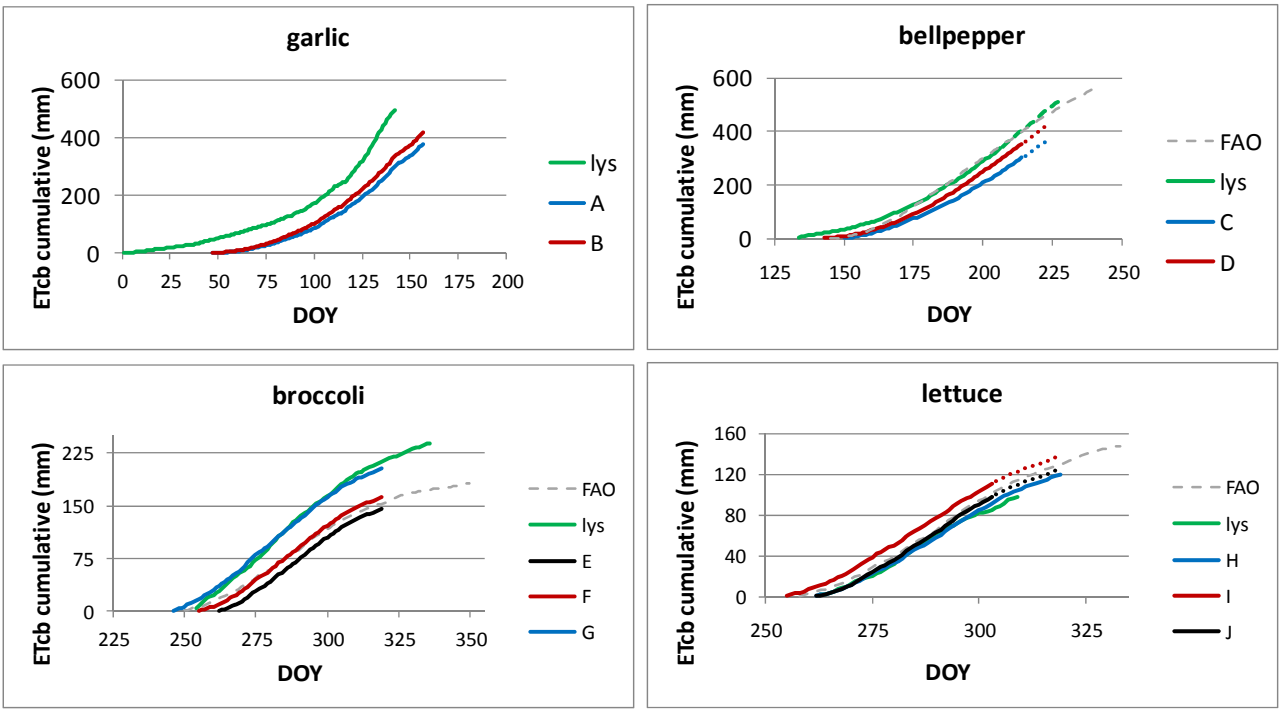

The RMS error of Equation (1), 0.062, causes ETcb retrieval uncertainties as shown in Table 5. Uncertainties on daily values for representative study fields are shown in absolute terms ranging from nil to 0.44 mm/d; seasonal uncertainties are presented in relative terms of range ±6–10%. Daily uncertainties are influenced by time of year, such that observations during periods of relatively low evaporative demand (ETo) result in lower uncertainty per given Fc error. Both daily and seasonal ETcb uncertainties are influenced by the shape of the Fc-Kcb curves defined by the Table 3 lysimeter equations. The broccoli and garlic curves show strong asymptotic behavior (see Figure 8 of [15]),

indicating that Kcb response saturates at Fc levels beyond what might be considered effective full cover. Satellite Fc errors during full canopy (mid-season) become less unimportant in such instances, to the point of irrelevance in the case of broccoli. The Fc-Kcb response functions for lettuce and bellpepper are more linear and thus remain sensitive to satellite Fc errors during mid-season. This effect is pronounced in seasonal uncertainty, with lower values (~6%) for broccoli and garlic as compared to lettuce and pepper (~10%). Additional uncertainty would be expected due to any error in Fc-Kcb conversion or ETo specification.

Table 4. Satellite observations of crop cycle duration from development start to harvest, and associated estimates of daily and total basal crop evapotranspiration. Total ETcb shown in terms of both water depth (mm) and volume (ML), which is a product of water depth and field size.

Field	Crop	Crop Duration (d)	ETcb Total (mm)	ETcb Total (ML)	Daily ETcb Mean (mm)	Daily ETcb Min (mm)	Daily ETcb Max (mm)
A	garlic	111[†]	378	113.4	3.5	0.4	8.9
B	garlic	111[†]	417	125.1	3.8	0.4	9.5
C	bellpepper	65–74	302–366	30.2–36.6	4.6	1.2	7.4
D	bellpepper	65–74	354–421	35.4–42.1	4.9	0.5	8.2
E	broccoli	>58[‡]	>146	>7.3	2.5	0.8	4.0
F	broccoli	>65[‡]	>162	>8.1	2.5	0.7	4.1
G	broccoli	>74[‡]	>203	>10.2	2.7	1.0	4.5
H	lettuce	>58[‡]	>120	>12.0	2.1	0.7	3.2
I	lettuce	49–65	110–138	11.0–13.8	2.1	0.8	3.4
J	lettuce	42–57	98–125	9.8–10.5	2.2	0.6	3.6

[†]through irrigation cutoff; [‡]incomplete growth cycle observed.

Table 5. ETcb retrieval uncertainties attributable to RMS error of NDVI-Fc Equation (1), for four study fields in 2008. Errors for daily ETcb are shown for DOY corresponding to the development stage with Fc near 50% of the maximum Fc shown on Figure 6, and during mid-season stage at maximum Fc.

Crop	Field	Daily ETcb Uncertainty, Development (mm); (DOY in paren's)	Daily ETcb Uncertainty, Mid-Season (mm); (DOY in paren's)	Seasonal ETcb Uncertainty
garlic	B	0.21 (091)	0.14 (134)	±5.9%
bellpepper	C	0.42 (178)	0.44 (214)	±9.5%
broccoli	F	0.26 (273)	~nil (319)	±6.1%
lettuce	J	0.31 (275)	0.16 (303)	±9.8%

4. Summary and Conclusions

Landsat Thematic Mapper reflective bands supported the estimation of basal crop evapotranspiration (ETcb) for several San Joaquin Valley (SJV) vegetable fields during 2008. Landsat-5 L1T terrain-corrected images were transformed to surface reflectance and converted to normalized difference vegetation index (NDVI) at 30 m spatial resolution. The NDVI was strongly related to green fractional cover across a broad variety of SJV annual and perennial crop types and maturity levels, and was used to estimate fractional cover over crop cycles of several study fields. Results from this portion of the study indicate that satellite NDVI can provide robust field-specific and regional estimates of Fc for specialty and other SJV crops, without need for crop type or supporting data or information beyond that needed for atmospheric correction. Prior relationships developed by weighing lysimeter were then used to convert fractional cover to basal crop coefficient. Finally, these coefficients were combined with reference evapotranspiration measurements from the California Irrigation Management Information System agricultural network to estimate basal crop evapotranspiration per overpass date. Temporal profiles of all variables were thus developed for four vegetable crops in several individual fields, along with estimates of daily and cumulative water use. Errors in satellite based fractional cover (Fc) estimation produced uncertainties of <0.5 mm/d for the crops examined here, with seasonal retrieval uncertainties of 6–10%. The results were compared with prior lysimeter experiments and FAO-56 planning guidelines.

The results then suggest that an optical satellite-based approach implemented in regions with an available reference ET (ETo) network, especially when combined with available 5–7 day ETo forecasts, may facilitate timely estimation of crop water use for support of resource monitoring and irrigation scheduling. While such observations can augment FAO-56 or other operational crop coefficient methods by monitoring actual crop development [30], resulting ETcb estimates must be supplemented with ancillary information to derive actual evapotranspiration (ETa) under conditions of crop water stress, which is not typically an issue for the high-value vegetable crops examined here excepting garlic during drydown. Extra information is required as well to account for soil surface evaporation resulting from irrigation operations or precipitation. Yet, compared with direct ETa estimation procedures that involve energy balance remote sensing [31], vegetation index methods are more approachable and can be less costly to implement [32]. Further, by avoiding the need for thermal imagery, vegetation index methods can potentially exploit viewing opportunities offered by a larger variety of satellite and airborne imaging systems [33] and can generate output at higher spatial resolution for use on smaller fields.

Future study might further address the extent to which texture or moisture related differences in soil reflectance affect NDVI based retrieval of Fc more broadly throughout SJV. Such study might explore the use of alternative vegetation indices that are less influenced by soil background such as the Soil Adjusted Vegetation Index and related transforms [34,35]. Among other things however, potential use of such indices in an operational context should be evaluated for cloud shadow sensitivity, where NDVI retrievals are fairly robust. Additional work could be done to quantify Fc and ETcb uncertainties related to presence of non-crop vegetation (cover crop, weeds). Such vegetation is not prevalent in SJV vegetable production, but might pose an important confusion factor with other crop

types at least at certain times of year. Further verification should be performed on mature orchards to evaluate conformity with the NDVI-Fc response function observed here.

Acknowledgments

Field support was provided by Jim Gartung (USDA-ARS). LEDAPS atmospheric correction processing was facilitated by the NASA Ames Ecological Forecasting Lab. We are grateful for cooperation of commercial growers at Tanimura & Antle, Red Rock Ranch, Britz, Terranova, and Harris Farms. The project was funded by the California Dept. Water Resources. LJ received additional support through NASA's Applied Sciences Program.

References

1. Calif. Dept. Food & Agriculture. *California Agricultural Production Statistics, Agricultural Resource Directory*; Available online: http://www.cdfa.ca.gov/statistics/ (accessed on 27 June 2011).
2. Temesgen, B.; Eching, S.; Davidoff, B.; Frame, K. Comparison of some reference evapotranspiration equations for California. *J. Irrig. Drain. Eng*. **2005**, *131*, 73-84.
3. Hart, Q.; Brugnach, M.; Temesgen, B.; Rueda, C.; Ustin, S.; Frame, K. Daily reference evapotranspiration for California using satellite imagery and weather station measurement interpolation. *Civil Eng. Environ. Syst*. **2009**, *26*, 19-33.
4. Allen, R.G.; Pereira, L.S.; Raes, D.; Smith, M. *Crop Evapotranspiration: Guidelines for Computing Crop Water Requirements*; FAO Irrigation and Drainage Paper # 56; UN Food & Agriculture Organization: Rome, Italy, 1998.
5. Bausch, W.C. Remote sensing of crop coefficients for improving the irrigation scheduling of corn. *Agr. Water Manage.* **1995**, *27*, 55-68.
6. Hunsaker, D.J.; Barnes, E.M.; Clarke, T.R.; Fitzgerald, G.J.; Pinter, P.J. Cotton irrigation scheduling using remotely sensed and FAO-56 basal crop coefficients. *ASAE Trans.* **2005**, *48*, 1395-1407.
7. Neale, C.M.U.; Jayanthi, H.; Wright, J.L. Irrigation water management using high resolution airborne remote sensing. *Irrig. Drain. Syst*. **2005**, *19*, 321-336.
8. Er-Raki, S.; Chehbouni, A.; Duchemin, G. Combining satellite remote sensing data with the FAO-56 dual approach for water use mapping in irrigated wheat fields of a semi-arid region. *Remote Sens*. **2010**, *2*, 375-387.
9. Grattan, S.R.; Bowers, W.; Dong, A.; Snyder, R.; Carroll, J.; George, W. New crop coefficients estimate water use of vegetables, row crops. *Calif. Agr.* **1998**, *52*, 16-21.
10. de Medeiros, G.; Arruda, F.B.; Sakai, E.; Fujiwara, M. The influence of crop canopy on evapotranspiration and crop coefficient of beans. *Agr. Water Manage.* **2001**, *49*, 211-224.
11. Ayars, J.E.; Johnson, R.S.; Phene, C.J.; Trout, T.J.; Clark, D.A.; Mead, R.M. Water use by drip-irrigated late-season peaches. *Irrig. Sci.* **2003**, *22*, 187-194.
12. Williams, L.E.; Ayars, J.E. Grapevine water use and crop coefficient are linear functions of shaded area beneath the canopy. *Agr. Forest Meteorol*. **2005**, *132*, 201-211.

13. Hanson, B.R.; May, D.M. Crop coefficients for drip-irrigated processing tomato. *Agr. Water Manage.* **2006**, *81*, 381-399.
14. Allen, R.G.; Pereira, L.S. Estimating crop coefficients from fraction of ground cover and height. *Irrig. Sci.* **2009**, *28*, 17-34.
15. Bryla, D.R.; Trout, T.J.; Ayars, J.E. Weighing lysimeters for developing crop coefficients and efficient irrigation practices for vegetable crops. *Hort. Sci.* **2010**, *45*, 1597-1604.
16. Asrar, G.; Fuchs, M.; Kanemasu, E.T.; Hatfield, J.L. Estimating absorbed photosynthetic radiation and leaf area index from spectral reflectance in wheat. *Agron. J.* **1984**, *76*, 300-306.
17. Daughtry, C.S.; Gallo, K.P.; Goward, S.N.; Prince, S.D.; Kustas, W.P. Spectral estimates of absorbed radiation and phytomass production in corn and soybean canopies. *Remote Sens. Environ*. **1992**, *39*, 141-152.
18. Goward, S.N.; Huemmrich, K.F. Vegetation canopy PAR absorptance and NDVI: An assessment using the SAIL model. *Remote Sens. Environ*. **1992**, *39*, 119-140.
19. Calera, A.; Martinez, C.; Melia, J. A procedure for obtaining green plant cover: Relation to NDVI in a case study for barley. *Int. J. Remote Sens*. **2001**, *22*, 3357-3362.
20. Johnson, L.F.; Scholasch, T. Remote sensing of shaded area in vineyards. *Hort. Tech*. **2005**, *15*, 859-863.
21. Lopez-Urrea, R.; Montoro, A.; Gonzalez-Piqueras, J.; Lopez-Fuster, P.; Fereres, E. Water use of spring wheat to raise water productivity. *Agr. Water Manage.* **2009**, *96*, 1305-1310.
22. Er-Raki, S.; Chehbouni, A.; Guemouria, N.; Duchemin, G.; Ezzahar, J.; Hadria, R. Combining FAO-56 model and ground-based remote sensing to estimate water consumptions of wheat crops in a semi-arid region. *Agr. Water Manage.* **2007**, *87*, 41-54.
23. Trout, T.J.; Johnson, L.F.; Gartung, J. Remote sensing of canopy cover in horticultural crops. *HortSci.* **2008**, *43*, 333-337.
24. Hornbuckle, J.W.; Car, N.J.; Christen, E.W.; Stein, T.M.; Williamson, B. *IrriSatSMS: Irrigation Water Management by Satellite and SMS—A Utilisation Framework*; CSIRO Land and Water Science Report No. 04/09; Commonwealth Scientific and Industrial Research Organisation: Griffith, NSW, Australia, 2009.
25. Masek, J.G.; Vermote, E.F.; El Saleous, N.Z.; Wolfe, R.; Hall, F.G.; Huemmrich, K.F.; Gao, F.; Kutler, J.; Lim, T. A Landsat surface reflectance dataset for North America, 1990–2000. *IEEE Trans. Geosci. Remote Sens. Lett.* **2006**, *3*, 68-72.
26. Vermote, E.F.; El Saleous, N.Z.; Justice, C.O. Atmospheric correction of MODIS data in the visible to middle infrared: first results. *Remote Sens. Environ.* **2002**, *83*, 97-111.
27. Kaufman, Y.J.; Wald, A.E.; Remer, L.A.; Gao, B.; Li, R.; Flynn, L. The MODIS 2.1-μm channel—Correlation with visible reflectance for use in remote sensing of aerosol. *IEEE Trans. Geosci. Remote Sens.* **1997**, *35*, 1286-1298.
28. Lillesand, T.; Kiefer, R. *Remote Sensing and Image Interpretation*, 3rd ed.; Wiley & Sons: New York, NY, USA, 1994; p. 18.
29. Ayars, J.E. Water requirement of irrigated garlic. *ASABE Trans*. **2008**, *51*, 1683-1688.
30. Rossi, S.; Rampini, A.; Bocchi, S. Boschetti, M. Operation monitoring of daily crop water requirements at the regional scale with time series of satellite data. *J. Irrig. Drain. Eng*. **2010**, *136*, 225-231.

31. Bastiaanssen, W.; Menenti, M.; Feddes, R.; Holtslag, A. A remote sensing surface energy balance algorithm for land (SEBAL). *J. Hydrol*. **1998**, *212*, 198-229.
32. Rafn, E.; Contor, B.; Ames, D. Evaluation of a method for estimating irrigated crop evapotranspiration coefficients from remotely sensed data in Idaho. *J. Irrig. Drain. Eng*. **2008**, *134*, 722-729.
33. Murray, R.S.; Nagler, P.L.; Morino, K.; Glenn, E.P. An empirical algorithm for estimating agricultural and riparian evapotranspiration using MODIS enhanced vegetation index and ground measurements of ET. II. Application to the Lower Colorado River, US. *Remote Sens*. **2009**, *1*, 1125-1138.
34. Bausch, W. Soil background effects on reflectance-based crop coefficients for corn. *Remote Sens. Environ*. **1993**, *46*, 213-222.
35. Montandon, L.; Small, E. The impact of soil reflectance on the quantification of green vegetation fraction from NDVI. *Remote Sens. Environ*. **2008**, *112*, 1835-1845.